AIAA JOURNAL
Vol. 33, No. 12, December 1995

Nonreflecting Boundary Conditions for Jet Flow Computations

M. Ehtesham Hayder* and Eli Turkel†
NASA Lewis Research Center, Cleveland, Ohio 44135

In this study, we examine the effect of boundary conditions, both inflow and outflow, on the predicted flow fluctuations in a supersonic jet entering into a subsonic outer flow. Various boundary conditions are used to compute the flowfield of a laminar axisymmetric jet excited at the inflow by a disturbance given by the corresponding eigenfunction of the linearized stability equations. Our goal is to determine the suitability of these conditions for computations of time-dependent flows. We solve the full time-dependent Navier–Stokes equations by a high-order numerical scheme. For very small excitations, the computed growth of the modes closely corresponds to that predicted by the linear theory. We then vary the excitation level and examine the effect of the boundary conditions in the nonlinear flow regime.

Nomenclature

a	= Riemann variable
c	= speed of sound
d, r	= distance from origin
E	= internal energy
F	= flux in x or z direction
G	= flux in y or r direction
L	= differential operator
M	= Mach number
m, n	= momentums
p	= pressure
Q	= solution vector
R, K	= characteristic variables
R, θ, ϕ	= spherical coordinate directions
r, θ, z	= polar coordinate directions
S	= source term
S_t	= Strouhal number
T	= temperature
t	= time
U	= mean axial velocity
u, v	= velocity components
x, y, z	= Cartesian coordinate direction
α	= growth rate
γ	= ratio of specific heats, 1.4
ϵ	= amplitude of excitation
θ	= momentum thickness
ρ	= density

I. Basic Scheme

We use a high-order extension of MacCormack's scheme, due to Gottlieb and Turkel,[1] to solve the Navier–Stokes equations. For the two-dimensional Navier–Stokes computations, the operator L in the equation $LQ = S$ or equivalently $Q_t + F_z + G_r = S$ is split into two one-dimensional operators, and the scheme is applied to these split operators. For the one-dimensional model/split equation $Q_t + F_z = S$, we express the predictor step with forward differences as

$$\bar{Q}_i = Q_i^n + \frac{\Delta t}{6\Delta z}\left\{7\left(F_{i+1}^n - F_i^n\right) - \left(F_{i+2}^n - F_{i+1}^n\right)\right\} + \Delta t S_i$$

and the corrector step with backward differences as

$$Q_i^{n+1} = \frac{1}{2}\left[\bar{Q}_i + Q_i^n + \frac{\Delta t}{6\Delta z}\{7(\bar{F}_i - \bar{F}_{i-1}) - (\bar{F}_{i-1} - \bar{F}_{i-2})\} + \Delta t S_i\right]$$

This scheme is second order accurate in time and becomes fourth order accurate in the spatial derivatives when alternated with symmetric variants.[1,2] This scheme has been extensively tested for accuracy[3,4] and compared with second-order and sixth-order accuracy in space. In addition it has been used by many other authors.[4–8] For our computations, the one-dimensional sweeps are arranged as

$$Q^{n+1} = L_{1z} L_{1r} Q^n$$

$$Q^{n+2} = L_{2r} L_{2z} Q^{n+1}$$

This scheme is used for the interior points. Interested readers may look into aforementioned references for more discussions on the accuracy of this scheme. To advance the scheme near boundaries the fluxes are extrapolated outside the domain to artificial points using a cubic extrapolation to compute the solution on the boundary. We then solve a set of equations (1) to get the solution at the new time for all boundary points. Hence, in all one-dimensional sweeps, the equations are updated based on the extrapolated fluxes when necessary. At the completion of a time step, i.e., a predictor and corrector in both one-dimensional sweeps, the boundary condition is imposed at both inflow, outflow, and the top boundary. The top boundary is a characteristic boundary and so is treated differently than the outflow boundary. We extrapolate three characteristics variables from the interior and set $p_t - \rho c v_t = 0$. In this study we concentrate on the effect of the outflow boundary condition and, to a lesser extent, on the inflow boundary treatment. We examine the effect of the boundary conditions near the shear layer. No geometric or corner effect is studied.

II. Outflow Boundary Conditions

The treatment of the outflow boundary condition is very important in getting an accurate solution of the Navier–Stokes equations. There have been many studies[9–13] attempting to minimize the reflections at the outflow boundary. These approaches are all based on the differential equation and do not account for features of the interior scheme. Standard theorems in numerical analysis guarantee (at least for the linearized equations) that the combined interior scheme plus boundary treatment is stable and accurate provided that certain conditions are met. The stability has been previously verified, while the accuracy demands that the boundary treatment be at least third order accurate in space. Many investigators base their approaches on linearized treatments of the differential equation. One could also develop nonlinear boundary conditions.[13,14] This will not be pursued in this study.

We are mainly interested in the viscous but high-Reynolds-number flow. The first question is whether the boundary treatment

Received Sept. 1, 1994; revision received May 14, 1995; accepted for publication May 14, 1995.

*Senior Research Associate, Institute for Computational Mechanics in Propulsion. Member AIAA.
†Institute for Computational Mechanics in Propulsion; currently Professor, Department of Mathematics, Tel-Aviv University, Tel-Aviv, Israel. Senior Member AIAA.

should be based on the Euler equations or the Navier–Stokes equations. The difference between the two approaches is not just the type of boundary conditions but even the number of boundary conditions that need to be externally given. For inviscid flow at inflow, when the flow is subsonic, one boundary condition needs to be specified corresponding to an incoming acoustic wave. For supersonic flow no boundary conditions are specified. For viscous flow the equations are no longer hyperbolic but rather incompletely parabolic. For subsonic flow four conditions need to be specified (in two dimensions), whereas for supersonic flow three conditions need to be specified. Moreover, for the inviscid (hyperbolic) case the needed boundary conditions should be of Dirichlet type; i.e., a combination of the dependent variables is specified. For the viscous problem (parabolic) the specified boundary condition can be either of Dirichlet type or Neumann type or a combination of both of these (Robin type). Many codes use inviscid type boundary conditions. This is based on the assumption that the flow in the far field is essentially inviscid because of the high Reynolds number and the lack of physical boundary layers. Indeed, specifying Dirichlet conditions in accordance with the parabolic theory would generate an artificial boundary layer. The number of Dirichlet boundary conditions in the far field should be chosen in accordance with hyperbolic theory. The rest of the variables should then have Neumann conditions or equivalently some extrapolation. See, for example, Hesthaven and Gottlieb.[15]

To be more specific we need to consider different types of configurations. For boundary-layer flows one needs to distinguish between the portion of the computational domain inside and outside the boundary layer. Outside the boundary layer one may be able to use inviscid type boundary conditions. Inside the boundary layer the pressure should be specified. Gustaffson and Nordstrom[16] have shown that the problem is also well posed if one extrapolates all of the variables inside the boundary layer. For external flow about an airfoil some codes use inviscid type conditions, whereas others extrapolate all of the variables. Though the flow seems to be inviscid in the far field, nevertheless viscous effects persist in the wake region. Thus, for example, there is a velocity defect no matter how far one goes downstream and the integral of this is constant. Thus, as one proceeds further downstream, the defect locally gets smaller but is spread over a larger region. This should affect the appropriate boundary conditions. In this paper we will consider jet flows. In these types of flows, viscous effects should be important near the shear layer even far downstream. A further complication that is most pronounced for shear flows is that one does not know the solution downstream and therefore one cannot impose any type of Dirichlet boundary condition. Frequently, there is a significant spreading of the shear layer, and so one does not know in advance even where the shear layer will intersect the outflow boundary. Furthermore, many theories expand the solution about a constant pressure in the far field and so obtain a differential equation for the pressure deviation. For shear flows the pressure differs on the two sides of the shear, and so the pressure is not constant in the far field except if the far-field boundary is extremely far away, which is not computationally practical. In other words, some of the nonreflecting boundary conditions that have been proposed in the literature are based on suppositions of the form of the outgoing wave, e.g., a plane wave or a spherical wave. However, these assumptions are not valid for shear flows. In spite of all these dangers we shall consider characteristic-like boundary conditions at outflow, and so the number of boundary conditions will be given by the inviscid theory. Nevertheless we shall see that viscous effects are at least partially accounted for. The main difficulty in implementing the correct outflow boundary conditions occurs for subsonic flows. For supersonic flows, all of the characteristics travel in the flow direction and boundary points can be calculated from known quantities at inflow or by extrapolation from the interior at outflow. For subsonic flow, one acoustic wave propagates against the flow direction. One condition is needed corresponding to this characteristic variable. The simplest approach is to linearize the equations and to use the one-dimensional characteristic variables normal to the surface. One then specifies the incoming characteristic variables and extrapolates the outgoing variables. Characteristic variables can also be obtained by solving differential equations instead of by extrapolation. For the acoustic waves one needs differential equations for $p_t \pm \rho c u_t$, where u is the velocity component normal to the boundary. For the shear wave one needs v_t, where v is tangential to the boundary and finally $p_t - c^2 \rho_t$ for the entropy variable. In this study, whenever the boundary condition is not specified but is free to float, then the appropriate characteristic variable is updated by the partial differential equation (except when mentioned explicitly). To avoid one-sided differences the fluxes are extrapolated outside the domain to artificial points using a cubic extrapolation. Whenever the appropriate combination is specified, we replace this by specifying the combination of the time derivatives. We can describe this as

$$\begin{aligned} p_t - \rho c u_t &= R_1 \\ p_t + \rho c u_t &= R_2 \\ p_t - c^2 \rho_t &= R_3 \\ v_t &= R_4 \end{aligned} \tag{1}$$

where R_i is determined by which variables are specified and which are not. Whenever the combination is not specified, R_i is just those spatial derivatives that come from the Navier–Stokes equations. Thus, R_i contains viscous contributions even though the basic format is based on inviscid characteristic theory. In implementing these differential equations we convert them to conservation variables $\rho, m = \rho u, n = \rho v$ and E. Assuming an ideal gas we then have

$$p_t = (\gamma - 1)\left(E_t + \frac{u^2 + v^2}{2}\rho_t - u m_t - v n_t\right)$$

$$u_t = \frac{m_t}{\rho} - \frac{u \rho_t}{\rho}$$

$$v_t = \frac{n_t}{\rho} - \frac{v \rho_t}{\rho}$$

For subsonic outflow we calculate R_2, R_3, and R_4 from the Navier–Stokes equations and set R_1 as prescribed by the given boundary condition. For supersonic flows, all of the R_i at the outflow boundary can be calculated from the Navier–Stokes equations or else by extrapolation of all of the characteristic variables from the interior.

A. Scott–Hankey Condition

Scott and Hankey[17] developed a condition to specify the incoming characteristic variable at the outflow, for the computation of unsteady flow in a transonic compressor rotor. Characteristic variables K_1–K_4 are defined as

$$K_1 = \frac{p}{\rho_\infty c_\infty} - u$$

$$K_2 = \frac{p}{\rho_\infty c_\infty} + u$$

$$K_3 = \rho - \frac{p}{c_\infty^2}$$

$$K_4 = v$$

At the outflow boundary K_2, K_3, and K_4 are extrapolated from the interior using

$$\frac{\partial K_2}{\partial z} = \frac{\partial K_3}{\partial z} = \frac{\partial K_4}{\partial z} = 0$$

The variable K_1 is specified at the exit boundary using p_{exit}, u_{exit}, p_∞, and u_∞; p_{exit} and u_{exit} are imposed in the inviscid region, and their axial derivatives are assumed to be zero in the viscous region. For this implementation, as in Scott et al.,[18] we assume p_{exit} and u_{exit} to be 99% of their inflow values at the small radial locations. For large radial locations p_{exit} and u_{exit} are assumed to be their values at the immediate interior point in the axial direction. We do not solve Eq. (1) when the Scott–Hankey condition is imposed.

B. One-Dimensional Characteristic Condition

The one-dimensional nonreflecting (characteristic) condition is $R_1 = 0$. This condition implies that the time derivative of the amplitude of the incoming characteristic wave is zero. This case is equivalent to the nonreflecting condition proposed by Thompson.[10] We have used this condition in previous studies.[2,19] For this case we found it more accurate to evaluate the boundary condition within the z sweeps, both predictor and corrector, rather than at the end of the entire time step. We refer to this implementation as the Thompson condition.

C. Giles' Condition

Giles[11] (and later Kroner[20]) added some tangential space derivatives in the outflow condition. He considers a wavelike solution of the form

$$U(x, y, t) = \exp[i(kx + ly - \omega t)]u^{\tau}$$

The boundary condition is derived by constructing a row vector v_n^L such that $v_n^L U = 0$ for each n corresponding to the incoming wave. Here we consider his second-order, two-dimensional, unsteady outflow condition. The equation for R_1 then becomes

$$p_t - \rho c u_t = -u\rho c v_y - v(p_y - \rho c u_y) = R_1$$

In polar coordinate we implement this as

$$p_t - \rho c u_t = -u\rho c \frac{(rv)_r}{r} - v\left[\frac{(rp)_r}{r} - \rho c \frac{(ru)_r}{r}\right] = R_1$$

This has the advantage of using only tangential derivatives at the outflow boundary, which are discretized by central differences.

D. Bayliss–Turkel Condition

Based on an asymptotic form of the wave equation, Bayliss and Turkel[12] derived a nonreflecting condition. They then used a change of variables to consider the case of a nonzero mean flow. Let $d^2 = [x^2/(1 - M^2)] + y^2$ where M is the Mach number, and x and y are the physical locations of the boundary point relative to some source. For jet flows this source is taken as the inflow. For other flows an appropriate center must be chosen. There is no reason, in general, to measure z and r from the origin of the local coordinate system. Then they got

$$\frac{1}{c\sqrt{1 - M^2}}\left[1 - \left(\frac{x}{d}\right)\frac{M}{\sqrt{1 - M^2}}\right]p_t + \left(\frac{x}{d}\right)p_x + \left(\frac{y}{d}\right)p_y + \frac{p - p_\infty}{2d} = 0$$

In three dimensions the inhomogeneous term is divided by d rather than the $2d$ (see two- and three-dimensional conditions by Roe[21]). For cylindrical coordinates (r, θ, z) multiply by d/r and use $x = r\cos(\theta)$, $y = r\sin(\theta)$ and the definition of d to get

$$\frac{s(\theta)}{c}p_t + \cos(\theta)p_x + \sin(\theta)p_y + \frac{p - p_\infty}{2r} = 0 \qquad (2)$$

where

$$s(\theta) = \frac{\sqrt{1 - M^2\sin^2(\theta)} - M\cos(\theta)}{1 - M^2}$$

Hariharan and Hagstrom[22] derived Eq. (2) as a boundary condition and noted its equivalence to the Bayliss–Turkel (see also Sec. II.G). Bayliss and Turkel then used the momentum equations to get p_x and p_y in terms of u_t and v_t and other spatial derivatives of u and v. Also assuming that $v_\infty = 0$ this yields

$$p_t - \rho c\frac{x}{d\sqrt{1 - M^2}}(u_t - uv_y) + c\sqrt{1 - M^2}\frac{y}{d}p_y + \frac{c\sqrt{1 - M^2}}{2d}(p - p_\infty) = 0$$

For many cases, the domain is much longer than it is high. Using $y \ll x$ we have a simplified form

$$p_t - \rho c u_t = -\rho c u v_y = R_1$$

In polar coordinates, we write the preceding equation as

$$p_t - \rho c u_t = -\rho c u\frac{(rv)_r}{r} = R_1$$

With this simplification we get an equation for the characteristic variable in a form similar to that proposed by Giles[11] but not identical with his condition. We will refer to this condition as the simplified Bayliss–Turkel condition.

We also consider another less simplified form of the Bayliss–Turkel boundary condition. We implemented this condition in our present axisymmetric jet computations as

$$p_t - \rho c u_t = -\rho c u\frac{(rv)_r}{r} - c\sqrt{1 - M^2}\frac{(rp)_r}{d} + \frac{c\sqrt{1 - M^2}}{d}(p - p_\infty) = R_1$$

In this study, we refer to this condition as the Bayliss–Turkel condition. The spatial derivatives are approximated by central differences.

E. Riemann Variables Condition

Hagstrom and Hariharan[14] derived a boundary condition by coupling the incoming and outgoing Riemann variables, a_1 and a_2,

$$a_1 = u + \frac{2c}{\gamma - 1}$$

$$a_2 = u - \frac{2c}{\gamma - 1}$$

where a_1 corresponds to the outgoing acoustic wave and a_2 corresponds to the incoming acoustic wave. Using asymptotic analysis in the far field in cylindrical coordinates, one gets

$$\left(u - \frac{2c}{\gamma - 1}\right)_t = \frac{c_\infty}{2z}\left[u - \frac{2(c - c_\infty)}{\gamma - 1}\right] = R_1$$

For this case we found it more accurate to evaluate the boundary condition within the z sweeps, both predictor and corrector, rather than at the end of the entire time step.

Instead of their full condition, we implement a one-dimensional version and use the preceding equation to calculate R_1. For convenience, we replace the equation for R_2 with

$$\left(u + \frac{2c}{\gamma - 1}\right)_t = R_2$$

It should be noted that this boundary condition was derived with the assumption that $u_\infty = 0$. As $z \to \infty$, $R_1 \to 0$ and this condition reduces to a one-dimensional characteristic condition equivalent to the one in Sec. II.B. Since c at the outflow has a profile, we choose the constant c_∞ based on the outflow at the top of the domain. The poor results for this scheme may be due to these choices for u_∞ and c_∞ and because we implemented a truncated version.

F. Roe's Condition

Roe[21] derived one boundary condition from the bicharacteristic equations as

$$(x - \beta M_\infty d)u_t + \beta^3 d c_\infty u_x + \beta^2 y[v_t + u_\infty v_x] + c_\infty(\beta d - M_\infty x)v_y = \frac{p - p_\infty}{2\rho_\infty}$$

where $\beta = \sqrt{(1 - M_\infty^2)}$ and d is as defined in Sec. II.D. This condition replaces the equation for R_1. For $x \gg y$, the preceding equation reduces to

$$u_t + c_\infty[(1 + M_\infty)u_x + v_y] = \frac{p - p_\infty}{2x\rho_\infty(1 - M_\infty)}$$

We further simply this equation by dropping the inhomogeneous term to get

$$u_t + c_\infty[(1 + M_\infty)u_x + v_y] = 0 \tag{3}$$

We implemented this condition and found the solution near the outflow to be oscillatory. We then made the following modification to improve this condition. We use the energy equation with $v = 0$,

$$p_t + up_x + \rho c^2(u_x + v_y) = 0$$

to convert Eq. (3) to

$$p_t - \rho c u_t = -up_x + \rho c^2 M u_x = R_1$$

The x derivatives are calculated by one-sided differences. We shall refer to this as Roe's condition.

G. Convective Pressure Condition

As pointed out before, Bayliss and Turkel developed a radiation condition for the wave equation based on an asymptotic form. This was generalized to the convective wave equation by a change of variables. The Bayliss and Turkel boundary condition was derived for two dimensions. Their pressure boundary condition was extended to three dimensions by Roe.[21] Later Hariharan and Hagstrom[22] developed an asymptotic expansion directly for the convective wave equation based on a Riemann function. Thus, in cylindrical coordinates (r, θ, z) with $R^2 = r^2 + z^2$

$$p \sim \sum_{j=0}^{\infty} \frac{F_j\{t - [R/U(\theta)]\theta\}}{R^{j+1}}$$

where

$$U(\theta) = u_\infty \cos\theta + c_\infty(1 - M^2 \sin\theta)^{\frac{1}{2}}$$

and $M = u_\infty/c_\infty$. The variable U is the inverse of $s(\theta)$ as given in Sec. II.D. This gave them a set of boundary conditions identical to the complete Bayliss–Turkel conditions, and in addition they were now able to prove uniform convergence to get improved error estimates. Tam and Webb[23] considered the linearized Euler equations. Using Fourier and Laplace transforms they independently derived the first term of the asymptotic expansion for the convective wave equation. They then derived an outflow boundary condition based on the far-field asymptotic solutions of the linearized Euler equations. Hence, the approaches of Bayliss–Turkel, Hariharan–Hagstrom, and Tam–Webb all yield the same equation. This is given in two dimensions by Eq. (2). While we have recast the nonreflecting boundary conditions in characteristic form, Tam and Webb considered Eq. (2) as an equation for the pressure and supplemented it by the linearized Euler equations for the density and the velocities.

In three-dimensional spherical coordinates, (R, θ, ϕ), Eq. (2) becomes

$$(p_t/U) + p_R + (p - p_\infty)/R = 0$$

We next transform from spherical to cylindrical coordinates. Then $p_R = p_r \cos(\theta) + p_z \sin(\theta)$ where $\sin(\theta) = z/R$ (note this is different than the cylindrical coordinate θ previously used). In this study, we consider a long domain with small height, i.e., $r \ll z$ or equivalently $R \sim z$, $\sin(\theta) \sim 1$. Thus,

$$p_t + (u + c)p_z + (p - p_\infty)/z = 0$$

where u is the axial velocity at the outflow boundary. In this paper we will refer to this condition as the simplified convective pressure condition.

H. Filtering

Besides nonreflecting boundary conditions based on the partial differential equation there are other approaches to remove the difficulties associated with far-field boundaries. One such approach was used by Colonius et al.,[24] who introduced a filter near the outflow. In this study, we examine the effect of filters for unsteady flow calculations. We choose a sixth-order filter of the form

$$\bar{f}_i = (1 - a)f_i + a\left[\frac{11}{16}f_i + \frac{15}{64}(f_{i+1} + f_{i-1}) - \frac{3}{32}(f_{i+2} + f_{i-2}) + \frac{1}{64}(f_{i+3} + f_{i-3})\right] \tag{4}$$

where $a = 0$ at the beginning of the filter (exit) zone and increases linearly to 1 at the outflow boundary.

III. Inflow Boundary Condition

For supersonic flow all characteristic variables propagate in the flow direction, and one can specify all the flow variables at the inflow. For subsonic flow, one characteristic variable propagates against the flow direction, and it needs to be extrapolated or estimated from the interior. Other conditions may be specified by the given inflow conditions. We specified the appropriate given inflow boundary conditions as the mean field plus a constant ϵ times a time-varying part based on the linear spatial stability theory eigenfunctions. If ϵ is sufficiently small, we expect the full Navier–Stokes equations to behave similar to the linear theory, at least for small distances from the inflow boundary.

A. BCI1: Extrapolate $p - \rho_0 c_0 u$

In this treatment, we extrapolate one characteristic variable (corresponding to the outgoing acoustic wave) from the interior and specify three conditions based on inflow conditions. We then use these four conditions to update all quantities at the inflow. In particular, we extrapolate $(p - \rho_0 c_0 u)$ from interior. We impose v and calculate $(p + \rho_0 c_0 u)$ and $(p - c_0^2 \rho)$ from the given inflow condition. The variables ρ_0 and c_0 are the linearized density and speed of sound at the inflow.

B. BCI2

In this case the inflow boundary condition is imposed using Eq. (1). We calculate R_1 from the solution of the Navier–Stokes equation at the inflow and calculate R_{2-4} from the given inflow condition. We then solve the preceding set of equations to get corrected time derivatives.

C. BCI3

Instead of specifying v as in the previous section, we can specify the normal derivative v_z. Since for small ϵ

$$v = \epsilon e^{\alpha z} Re[V(r)e^{i\omega t}]$$

v_z at inflow $(z = 0)$ is given by

$$v_z = \epsilon \alpha Re[V(r)e^{i\omega t}]$$

This boundary condition is weaker in that we supply derivative information rather than the v component directly, and so v can shift by a function of time. On the other hand we are supplying additional information on the growth rate α, which is lacking in the other boundary conditions. When the linear eigenfunction is not known, one can sometimes specify the vorticity as suggested by Roe.[21]

IV. Results

We first investigate the effect of the outflow boundary conditions for unsteady jet simulations in axisymmetric coordinates (z, r). We excite the flow at the inflow with the eigenfunctions of the linearized stability equations. Discussions on eigenfunctions of the linearized equations may be found in Scott et al.[18] Some details of the development of the flow for the present class of problem is given by Hayder et al.[19] Because of its importance in sound source computation, we examine the growth of the pressure disturbance downstream. We are interested in a supersonic jet flowing in a subsonic freestream. We vary the inflow excitation and see the effect of the boundary conditions for both the linear and nonlinear regime of the flow.

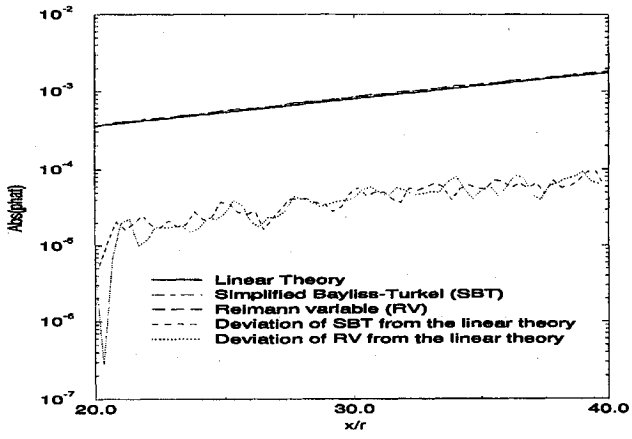

Fig. 1a Comparison of the linear theory prediction with numerical solutions.

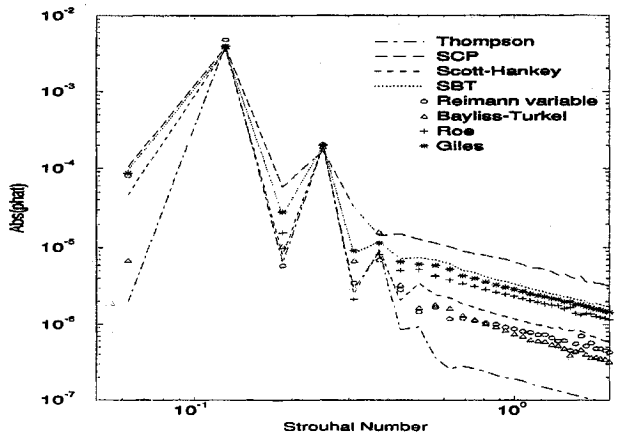

Fig. 1b Pressure spectra at outflow for $\epsilon = 2.5 \times 10^{-4}$.

We consider a jet with the mean inflow profile

$$\bar{U}_r = U_\infty + (U_c - U_\infty) g_r$$

$$\bar{T}_r = T_c + (T_\infty - T_c) g_r + \frac{\gamma - 1}{2} M_c^2 (1 - g_r) g_r \qquad (5)$$

$$g_r = \frac{1}{2}\left\{1 + \tanh\left[\frac{(1/r) - r}{4\theta}\right]\right\}$$

where θ is the momentum thickness. The subscripts c and ∞ refer to the centerline and freestream values, respectively. At inflow, we assume the radial velocity is zero and the static pressure is constant. The standard size of our computational domain is 50 radii in the axial and 5 radii in the radial directions, respectively. We excite the inflow profile at location r and time t as

$$U(r,t) = \bar{U}(r) + \epsilon Re(\hat{U} e^{i\pi S_t t})$$

$$P(r,t) = \bar{P}(r) + \epsilon Re(\hat{P} e^{i\pi S_t t})$$

$$\rho(r,t) = \bar{\rho}(r) + \epsilon Re(\hat{\rho} e^{i\pi S_t t})$$

$$V(r,t) = \epsilon Re(\hat{V} e^{i\pi S_t t})$$

where $\hat{U}$, $\hat{V}$, $\hat{\rho}$, and $\hat{P}$ are the eigenfunctions of the linearized equations with the same mean flow profile. The variable ϵ is the excitation level. For small ϵ the growth of the disturbance modes should agree with that predicted by the linearized Euler equations.

We consider a case with $U_\infty/U_c = \frac{1}{4}$, $T_\infty/T_c = \frac{1}{2}$, momentum thickness $\theta = \frac{1}{8}$, and Strouhal number $S_t = \frac{1}{8}$. The jet center Mach number is 1.5, whereas the Reynolds number based on the jet diameter is 1.2×10^6. Unless otherwise mentioned, the axial

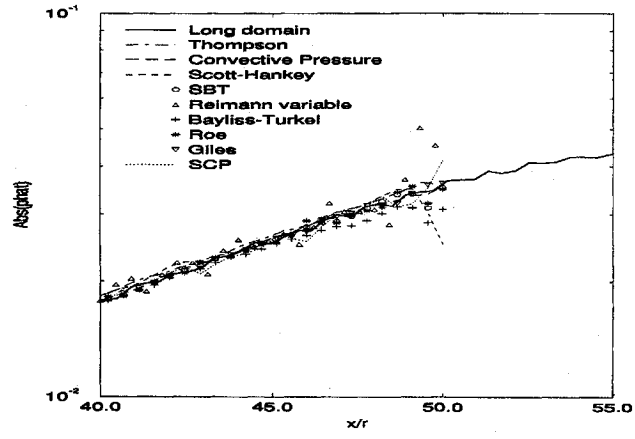

Fig. 2 Amplitude of pressure oscillations ($|\hat{P}|$) for $\epsilon = 2.5 \times 10^{-3}$.

variation of the disturbances correspond to $S_t = \frac{1}{8}$ at the jet edge ($r = 1$). This also corresponds to the excitation frequency in the simulations. Pressure disturbances in this study are calculated by a discrete Fourier transform in time and so they are functions of z:

$$|\hat{P}_k| = \left| 2 \sum_{j=0}^{n-1} P_j e^{\frac{i2\pi jk}{n}} \right|$$

We examine the effects of the different outflow conditions presented in Sec. II. We use three values of ϵ, 2.5×10^{-4}, 2.5×10^{-3}, and 5.0×10^{-3} and call them low, moderate, and high excitation levels, respectively. These excitation levels were chosen after numerical experiments to show linear, intermediate, and nonlinear effects on the growth of the disturbance. Computations with low level of disturbances were done with a 300×120 grid. For low excitation level, computed growth of the pressure disturbance ($|\hat{P}|$) compares well with the prediction of the linear theory. However, as shown in Fig. 1a the numerical solutions slightly oscillate and deviate from the prediction of the linear theory. Deviation from the linear theory could come from the nonlinear effects. Boundary treatments could lead to unphysical oscillations, which a high-order algorithm like our present scheme may retain in the numerical solution. The variable $|\hat{P}|$ is the absolute value of the Fourier transform of pressure in time at $S_t = \frac{1}{8}$ along the jet edge ($r = 1$). Our interior scheme is spatially fourth order accurate. Since we kept the same interior scheme for all of our tests, any difference in the solutions near the boundary should primarily be caused by the boundary conditions and their implementations. Since the disturbance level is low, as expected computed solutions are close to the prediction of the linear theory. In Fig. 1b the spectra of the pressure disturbance at the outflow boundary is shown. Only discrete points in x are calculated. They are connected by a straight line only to increase visualization.

We next consider computations for $\epsilon = 2.5 \times 10^{-3}$ with a 225×150 grid. In Fig. 2 we compare the solutions in the standard domain (50 radii long) with the solution in an extended domain (80 radii long). For this ϵ, the boundary condition effects are noticeable; however, $|\hat{P}|$ still shows linear growth. The Riemann variable condition shows more oscillations near the outflow than the other conditions. Finally, we excite the inflow with the high excitation level, $\epsilon = 5 \times 10^{-3}$. We again used the standard and the extended domain as described earlier. We use a 400×100 grid for the extended domain and show $|\hat{P}|$ in Figs. 3a and 3b. For this level of excitation, we observe a linear growth of pressure oscillations near the inflow and decay of such oscillations due to nonlinear effects near the outflow. Since we used discrete Fourier transform, some unresolved frequency contribution may appear as oscillations in $|\hat{P}|$. In Fig. 3a we show $|\hat{P}|$ for three different time windows with the convective pressure boundary condition and observe such differences in the solution near the outflow boundary due to unresolved low-frequency oscillations. Since different outflow boundary conditions yield essentially identical results away from the outflow boundary, oscillations in these places are not likely due to the treatments of

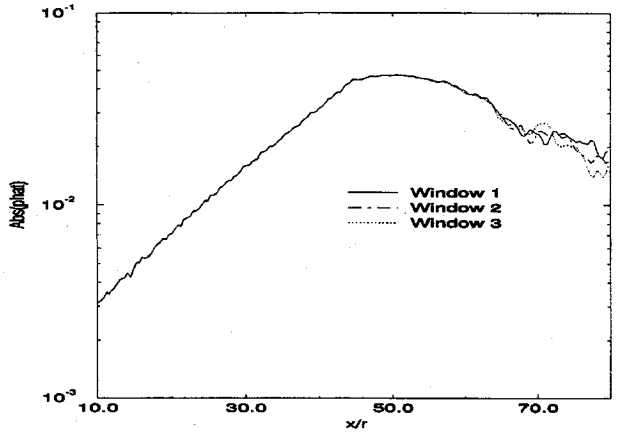

Fig. 3a Comparison of $|\hat{P}|$ at different time windows.

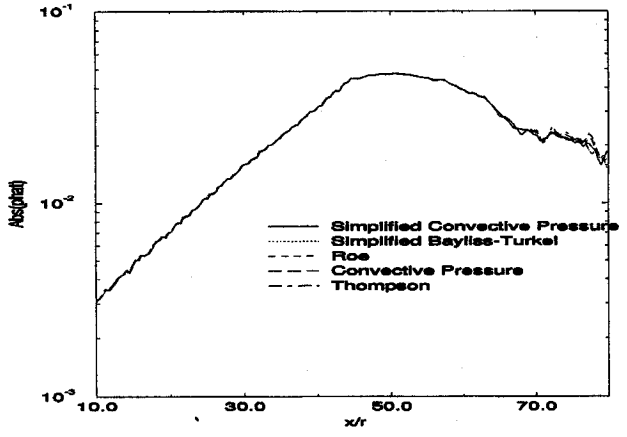

Fig. 3b $|\hat{P}|$ in long domain solutions for $\epsilon = 5 \times 10^{-3}$.

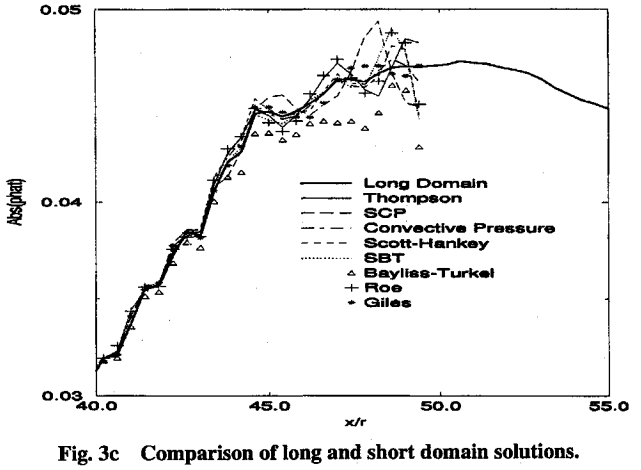

Fig. 3c Comparison of long and short domain solutions.

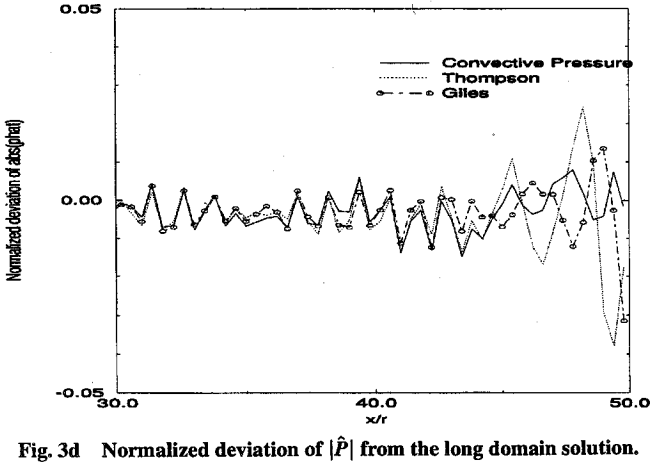

Fig. 3d Normalized deviation of $|\hat{P}|$ from the long domain solution.

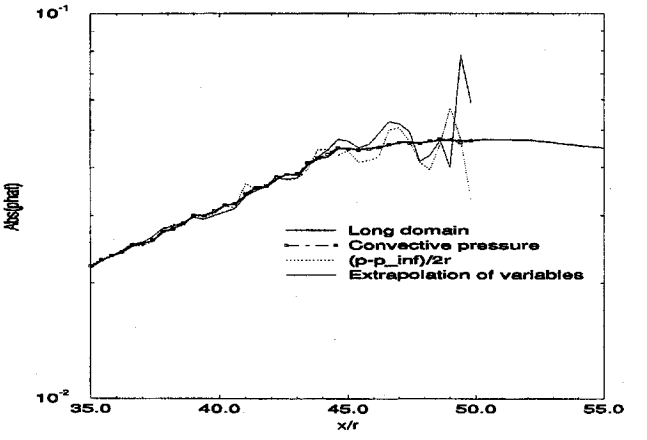

Fig. 4 Comparison of implementation alternatives.

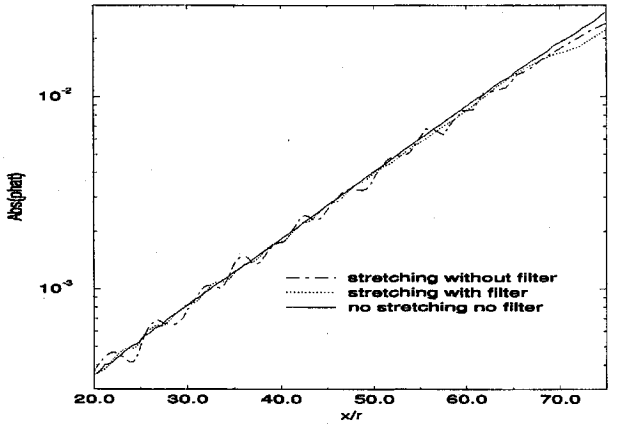

Fig. 5 Amplitude of pressure oscillations ($|\hat{P}|$) in exit layer simulations.

outflow boundary. In Fig. 3b all five boundary conditions essentially reproduced most of the oscillations away from the outflow boundary. In Fig. 3c, we compare solutions with different outflow boundary conditions with the long domain solution. The convective pressure, Giles and Thompson conditions were the most accurate near the outflow boundary, and we plot the normalized deviation of $|\hat{P}|$ in these solutions from the long domain solution in Fig. 3d. Normalization was done by $|\hat{P}|$ of the long domain at the corresponding axial location. In Fig. 4 we examine two alternate ideas in our implementations of the boundary conditions. Tests are done at $\epsilon = 5 \times 10^{-3}$. Results of these two formulations are compared against the result with the convective pressure condition. First we examine the type of extrapolations at the boundary. For our usual calculations, we extrapolate fluxes at the boundary to get values at ghost points. Alternatively, one could extrapolate variables and then calculate fluxes. For the present flow conditions and numerical parameters, we see the extrapolation of fluxes gives less oscillatory results. Next we examine a variation in the implementation of the convective pressure condition for our axisymmetric jet computations. We used r instead of $2r$ in Eq. (2) (see discussion in Sec. II.D). One needs to use factor r in three-dimensional flow computations. As shown in the Fig. 4, the result with the factor $2r$ shows oscillations, which are almost absent for the factor r (convective pressure).

We next examine the effect of an exit layer. This was used by Colonius et al.[24] We will examine the concept but will use a different stretching and filter. We consider three cases. In the first case, we use a 300 × 120 grid for the standard domain and add 60 grid points in the axial direction with stretching. We refer to these extra points as the exit layer. We use an $x^{1.5}$ stretching in this exit layer. Including the exit layer the computational domain is about 75 radii long and 5 radii high. In the second case, we add a filter [Eq. (4)] in the exit layer. In the third case, we compute the solution in the longer domain but with a 450 × 120 grid. We refer this solution as the "no stretching, no filter" case. We use a low excitation level ($\epsilon = 2.5 \times 10^{-4}$) for the exit layer study. The comparison of $|\hat{P}|$ is shown in Fig. 5. We observe pressure oscillations that are introduced

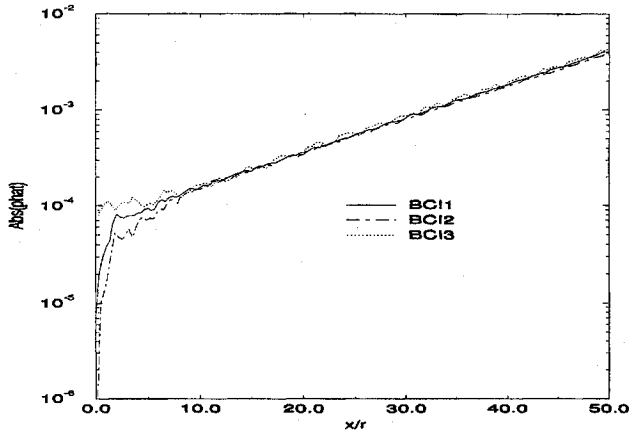

Fig. 6 Comparison of inflow boundary conditions.

by the stretching. These oscillations propagate into the interior from the exit layer. With filtering these oscillations are reduced.

In Fig. 6 we compare the solutions for three inflow conditions. For conditions BCI1 and BCI2 there is an adjustment region of about 4 jet diameters. The solutions downstream are not affected by this. Nevertheless, we do not expect any adjustment region since we are forcing the solution with the linear eigenfunctions. The width of this adjustment region remains the same when we refine the grid. Hence, this is not a purely numerical artifact. If we specify the normal derivative of v as given in BCI3, we considerably reduce this adjustment region but at the expense of increased oscillations in the domain. The improvement when specifying v_z may be because we are including the growth rate α in the boundary condition. We obtained similar results by enforcing vorticity instead of v at the inflow.

V. Conclusions

In the tests performed, for a supersonic jet flow entering a subsonic ambient media, the best outflow boundary condition seems to be the convective pressure condition. The simplifications introduced by Bayliss and Turkel when they derived their final condition reduce the accuracy. The boundary condition suggested by Giles was comparable to that of the convective pressure condition. These boundary conditions were implemented after a complete time step with all intermediate steps using third-order extrapolation of the fluxes. Using the differential equations based on one-dimensional characteristics was equally good if this was incorporated in all of the z sweeps and not just done at the end of the entire time step. All of these conditions closely followed the long domain solution except for small oscillations in the final 10% of the domain. Hence, one should add a small region (about 10% for the present flow conditions) beyond the domain of interest, and then any of these conditions can be used. The other conditions showed larger deviations at the outflow but were still useful. Stretching the mesh at the outflow introduced oscillations that were reduced by filtering.

The inflow for the subsonic/supersonic case exhibited an adjustment region until the linear growth rate was achieved even though the linear eigenfunctions were used for the inflow data. The size of this adjustment region was mesh independent. For the supersonic/supersonic flow, oscillations were observed further down the jet and also appeared to be independent of the mesh. When the v_z (or vorticity) was specified, the results for the supersonic/subsonic flow agreed better with linear theory with a smaller adjustment region. This may be because specifying v_z gives additional information about the growth rate. However, because only derivative information is given, the resultant solution was less smooth.

For both inflow and outflow there is need to determine whether it is better to impose the boundary conditions within the sweeps or to impose the boundary conditions only at the conclusion of an entire time step. The boundary condition equations may need to be split to implement within the sweeps. In this study, the one-dimensional characteristics (Thompson) and the Riemann variable conditions were both better when used within the sweeps. Both these conditions do not involve any spatial derivatives.

References

[1]Gottlieb, D., and Turkel, E., "Dissipative Two-Four Methods for Time Dependent Problems," *Mathematics of Computation*, Vol. 30, 1976, pp. 703–723.

[2]Hayder, M. E., and Turkel, E., "High Order Accurate Solutions of Viscous Problems," AIAA Paper 93-3074, 1993.

[3]Bayliss, A., Maestrello, L., Parikh, P., and Turkel, E., "A Fourth Order Method for the Unsteady Compressible Navier–Stokes Equations," AIAA Paper 85-1694, 1985.

[4]Sankar, L. N., Reddy, N. N., and Hariharan, N. "A Comparative Study of Numerical Schemes for Aero-Acoustic Applications," *FED—Vol. 147, Computational Aero- and Hydro-Acoustics*, American Society of Mechanical Engineers, 1993, pp. 35–40.

[5]Farouk, B., Oran, E. S., and Kailasanath, K., "Numerical Simulations of the Structure of Supersonic Shear Layers," *Physics of Fluids A*, Vol. 3, 1991, pp. 2786–2798.

[6]Frendi, A., Maestrello, L., and Bayliss, A., "Coupling between Plate Vibration and Acoustic Radiation," *Journal of Sound and Vibration*, Vol. 177, 1994, pp. 207–226.

[7]Maestrello, L., Bayliss, A., and Krishnan, R., "On the Interaction between First- and Second-Mode Waves in a Supersonic Boundary Layer," *Physics of Fluids A*, Vol. 3, 1991, pp. 3014–3020.

[8]Ragab, S. A., and Sheen, S., "The Nonlinear Development of Supersonic Instability Waves in a Mixing Layer," *Physics of Fluids A*, Vol. 4, 1991, pp. 553–566.

[9]Engquist, B., and Majda, A., "Absorbing Boundary Conditions for the Numerical Simulation of Waves," *Mathematics of Computations*, Vol. 31, No. 139, 1977, pp. 629–651.

[10]Thompson, K. W., "Time Dependent Boundary Conditions for Hyperbolic System, II," *Journal of Computational Physics*," Vol. 89, 1990, pp. 439–461.

[11]Giles, M. G., "Nonreflecting Boundary Conditions for Euler Equations Calculations," *AIAA Journal*, Vol. 28, 1990, pp. 2050–2058.

[12]Bayliss, A., and Turkel, E., "Far Field Boundary Condition for Compressible Flows," *Journal of Computational Physics*, Vol. 48, 1982, pp. 182–199.

[13]Atkins, H., and Casper, J., "Nonreflecting Boundary Conditions for High-Order Methods," *AIAA Journal*, Vol. 32, No. 3, 1994, pp. 512–518.

[14]Hagstrom, T., and Hariharan, S. I., "Accurate Boundary Conditions for Exterior Problems in Gas Dynamics," *Mathematics of Computation*, Vol. 51, No. 184, 1988, pp. 581–592.

[15]Hesthaven, J. S., and Gottlieb, D., "A Stable Penalty Method for the Compressible Navier–Stokes Equations. I. Open Boundary Conditions," ICASE Rept. 94-68, 1994.

[16]Gustaffson, B., and Nordstrom, J., "Extrapolation Procedures at Outflow Boundaries for the Navier–Stokes Equations," *Comp. Meth. in Appl. Sciences and Engineering*, edited by Glowinski and Lichnewsky, SIAM Publishers, 1990, pp. 136–150.

[17]Scott, J. N., and Hankey, W. L., "Boundary Condition for Navier–Stokes Solutions of Unsteady Flow in a Compressor Rotor," *Three-Dimensional Flow Phenomena in Fluid Machinery*, Vol. 32, American Society of Mechanical Engineers, New York, 1985.

[18]Scott, J. N., Mankbadi, R. R., Hayder, M. E., and Hariharan, S. I., "Outflow Boundary Conditions for the Computational Analysis of Jet Noise," AIAA Paper 93-4366, Oct. 1993.

[19]Hayder, M. E., Turkel, E., and Mankbadi, R. R., "Numerical Simulations of a High Mach Number Jet Flow," AIAA Paper 93-0653, 1993.

[20]Kroner, D., "Absorbing Boundary Conditions for the Linearized Euler Equations in 2-D," *Mathematics of Computation*, Vol. 57, 1991, pp. 153–167.

[21]Roe, P. L., "Remote Boundary Conditions for Unsteady Multidimensional Aerodynamic Computations," *Computer and Fluids Journal*, Vol. 17, No. 1, 1989, pp. 221–231.

[22]Hariharan, S. I., and Hagstrom, T., "Far Field Expansion for Anisotropic Wave Equations," *Computational Acoustics (IMACS)*, Vol. 2, edited by Lee, Cakmak, and Vichnevetsky, Elsvier, 1990, pp. 283–294.

[23]Tam, C. K. W., and Webb, J. C., "Dispersion-Relation-Preserving Finite Difference Schemes for Computational Acoustics," *Journal of Computational Physics*, Vol. 107, 1993, pp. 262–281.

[24]Colonius, T., Lele, S. K., and Moin, P., "Boundary Conditions for Direct Computations of Aerodynamic Sound Generation," AIAA Paper 92-02-075, 1992.